

# Hyperbaric oxygen induces a cytoprotective and angiogenic response in human microvascular endothelial cells

Cassandra A. Godman · Kousanee P. Chheda ·  
Lawrence E. Hightower · George Perdrizet ·  
Dong-Guk Shin · Charles Giardina

Received: 17 September 2009 / Revised: 2 November 2009 / Accepted: 4 November 2009 / Published online: 1 December 2009  
© Cell Stress Society International 2009

**Abstract** A genome-wide microarray analysis of gene expression was carried out on human microvascular endothelial cells (HMEC-1) exposed to hyperbaric oxygen treatment (HBOT) under conditions that approximated clinical settings. Highly up-regulated genes included immediate early transcription factors (FOS, FOSB, and JUNB) and metallothioneins. Six molecular chaperones were also up-regulated immediately following HBOT, and all of these have been implicated in protein damage control. Pathway analysis programs identified the Nrf2-mediated oxidative stress response as one of the primary responders to HBOT. Several of the microarray changes in the Nrf2 pathway and a molecular chaperone were validated using quantitative PCR. For all of the genes tested (Nrf2, HMOX1, HSPA1A, M1A, ACTC1, and FOS), HBOT elicited large responses, whereas changes were minimal following treatment with 100% O<sub>2</sub> in the absence of elevated pressure. The increased expression of immediate early and cytoprotective genes corresponded with an

HBOT-induced increase in cell proliferation and oxidative stress resistance. In addition, HBOT treatment enhanced endothelial tube formation on Matrigel plates, with particularly dramatic effects observed following two daily HBO treatments. Understanding how HBOT influences gene expression changes in endothelial cells may be beneficial for improving current HBOT-based wound-healing protocols. These data also point to other potential HBOT applications where stimulating protection and repair of the endothelium would be beneficial, such as patient preconditioning prior to major surgery.

**Keywords** Hyperbaric oxygen · Microarray · HMEC-1 · Cytoprotection · Antioxidant

## Introduction

Hyperbaric oxygen therapy (HBOT) involves the administration of 100% O<sub>2</sub> at pressures above 1 atm (Thom 2009). Currently, the Undersea and Hyperbaric Medical Society has defined 13 indications for which HBOT is approved including air/gas embolisms, CO poisoning, acute traumatic ischemias, and chronic wounds (Gesell 2008). In fact, HBOT is widely used for the treatment of diabetic ulcers (Duzgun et al. 2008; Liu and Velazquez 2008; Ong 2008; Thackham et al. 2008; Efrati et al. 2009), an application that will only increase as the population ages. One way HBOT acts to enhance chronic wound healing is by stimulating angiogenesis (Ren et al. 2008; Milovanova et al. 2009; Sander et al. 2009; Yuan et al. 2009). The tissue responsible for angiogenesis, the vascular endothelium, has been the topic of several studies to determine the mechanisms of the beneficial effects of HBO. In one proposed mechanism, HBO increases the partial pressure of

**Electronic supplementary material** The online version of this article (doi:10.1007/s12192-009-0159-0) contains supplementary material, which is available to authorized users.

C. A. Godman (✉) · K. P. Chheda · L. E. Hightower · C. Giardina  
Department of Molecular and Cell Biology,  
University of Connecticut,  
Storrs, CT, USA  
e-mail: Cassandra.Godman@uconn.edu

G. Perdrizet  
Department of Surgery, Morristown Memorial Hospital,  
Morristown, NJ, USA

D.-G. Shin  
Department of Computer Science and Engineering,  
University of Connecticut,  
Storrs, CT, USA

oxygen in circulating plasma, which helps to stimulate oxygen-dependent collagen matrix formation, a crucial step in wound healing (Gurdol et al. 2009). It has also been shown that seven daily HBO treatments can decrease hypoxia inducible factor 1 alpha expression in rat ischemic wound tissue, thereby attenuating apoptosis. Furthermore, this report demonstrated a reduction in the numbers of neutrophils present at the wound site following HBOT, indicative of a reduction in inflammation (Zhang et al. 2008).

Different gene and protein expression changes have been identified following HBOT in various experimental systems. For example, Lin et al. described how HBOT can specifically induce angiopoietin-2 in human umbilical vein endothelial cells, a protein that can stimulate angiogenesis when expressed coordinately with vascular endothelial growth factor. In humans as well as cell culture models, HBOT has also been shown to induce expression of heme oxygenase-1 (HMOX1), a protein that protects cells against oxidative stress (Speit et al. 2000; Rothfuss and Speit 2002; Li et al. 2007). This finding supports the potential efficacy of HBOT as a preconditioning therapy that would help increase tolerance against various injuries, particularly those that involve an oxidative stress component. Such preconditioning could be performed prior to a surgery that carries the risk of an ischemia/reperfusion event.

Our present study takes a genome-wide approach to obtain insight into potential mechanisms of HBO action in vascular endothelial cells. An Illumina bead array analysis was performed on human microvascular endothelial cells (HMEC-1) treated with HBO under conditions that approximated clinical settings. RNA expression was assessed in cells immediately and 24 h following HBO exposure. We identified 8,181 genes that were significantly changed in at least one treatment group. Analysis revealed both up- and down-regulation of gene expression with changes observed in antioxidant response pathways, molecular chaperone expression, and immediate early genes. To our knowledge, this is the first report of microarray analysis on HBO-treated human dermal microvascular endothelial cells. In general, our findings support strong antioxidant and pro-survival effects of HBO on endothelial cells, clarify mechanisms of action for present clinical HBO applications, and suggest new therapeutic applications.

## Materials and methods

### Cell culture and treatments

HMEC-1 were obtained from the Center for Disease Control and Prevention (Atlanta, GA). These cells have been immortalized by the SV40 large T antigen driven by

the Rous Sarcoma Virus long terminal repeat (Ades et al. 1992). They retain the morphology, phenotype, and functional characteristics of normal HMEC-1. Cells were cultured in MCDB 131 media (Invitrogen) supplemented with 10% fetal bovine serum (Lonza), 1% antibiotic/antimycotic (Gibco), human epidermal growth factor (10 ng/ml), and hydrocortisone (Sigma, 1 µg/ml) and maintained in a humidified incubator at 37°C and 5% CO<sub>2</sub>. *t*-Butyl hydroperoxide (Sigma) was diluted in sterile water to indicated concentrations immediately before treatment.

### Hyperbaric oxygen treatment

Experimental treatment was performed using an OxyCure 3000 hyperbaric incubator (OxyHeal Health Group) at 100% O<sub>2</sub> at 2.4 atm, at 37°C for 60 min. For the duration of the treatment, culture media was replaced with CO<sub>2</sub>-independent media (Gibco). Immediately following treatment, cells were either returned to normal complete media and culture conditions for recovery or processed immediately for RNA analysis. HBO treatment conditions were chosen to mimic current human treatment protocols.

### RNA isolation and microarray data analysis

RNA was isolated using Trizol reagent according to the manufacturer's instructions (Invitrogen) as previously reported (Godman et al. 2008) Briefly, culture media was removed, and Trizol reagent was added followed by chloroform extraction and isopropanol precipitation. The concentration of resulting RNA was determined using spectrophotometric methods. RNA was stored at -80°C.

### Microarray data preprocessing and selection of differentially expressed genes

After hybridization, the Illumina HumanWG-6 BeadChip was analyzed by the Gene Expression Module of BeadStudio Software (Illumina). Raw intensity and present/absent call of each probe was obtained for the six hybridized samples and exported in a single comma-separated file. We used the R (Ihaka and Gentleman 1996) and BioConductor Lumi packages (Du et al. 2008) to examine the quality control information and perform preprocessing on the raw data. Variance stabilizing transformation (VST) and robust spline normalization were applied on the raw data to generate normalized and comparable data among samples. After normalization, we used inverse VST to transform intensity data back to the raw scale before computing ratios between samples. Complete gene expression data are available in the Gene Expression Omnibus at <http://www.ncbi.nlm.nih.gov/geo/>.

### Pattern-based clustering

We used pattern-based clustering as an approach to perform functional analysis by grouping genes with similar expression patterns. Pattern-based clustering uses non-numeric parameters assigned for each fold change pattern to group genes in order to avoid assigning a predefined clustering number and to avoid common inconsistency problems in distance-based clustering algorithms such as *K* means.

We arranged the samples in the order of control 0-h time point (CTRL0), HBOT 0-h time point (HBOT0), control 24-h time point (CTRL24), and HBOT 24-h time point (HBOT24) for pattern-based clustering so that adjacent samples share only one variable. The genes that we used for pattern-based clustering are the union of the differentially expressed genes selected from the three comparisons: HBOT0 vs. CTRL0, HBOT24 vs. CTRL24, and HBOT24 vs. HBOT0. This union set contains genes that are regulated in at least one of the three comparisons and meets the minimum requirement to be included for clustering analysis.

### Ingenuity Pathway Analysis

Canonical pathway and gene function analyses were executed using Ingenuity Pathways Analysis tools (Ingenuity Systems, Mountain View, CA), a web-delivered application that enables the discovery, visualization, and exploration of molecular interaction networks in gene expression data. We selected genes with a fold change above 1.25 and below 0.75 for each comparison (HBOT0/CTRL0 and HBOT24/CTRL24) to be uploaded into the Ingenuity Pathway Analysis. Significances for biological functions or canonical pathways were assigned to each network by determining a *p* value for the enrichment of the genes in the network for such functions or pathways compared with the entire Ingenuity pathway knowledge base as a reference set. Right-tailed Fisher's exact test was used with  $p \leq 0.001$ . The choice of *p* value dramatically affects the output of the pathway analysis tools. For example, inclusion of the entire data set resulted in the selection of the Nrf2 oxidative stress pathway, ERK/MAPK pathway, and Integrin pathway as highly affected, based on the number of gene expression changes, but not statistically significant. Therefore, we tested a series of fold-change cutoffs to include in the analysis in order to produce statistically significant *p* values. As a control, we compared the untreated samples from each time point to each other and found no significant changes present using cutoff values that generated a  $p \leq 0.001$ .

### Reverse transcription PCR and quantitative real-time PCR

For reverse transcription PCR, 1–2  $\mu\text{g}$  of RNA was diluted in water and combined according to manufacturer's

instructions with the Applied Biosystems High Capacity cDNA Reverse Transcription Kit (Foster City, CA). Real-Time PCR was performed using an Applied Biosystems 7300 Real-Time PCR system and software. Reactions were run for 40 cycles with the TaqMan 2 $\times$  Universal PCR Master Mix in 10  $\mu\text{l}$  volumes with approximately 12.5 ng cDNA. TaqMan gene expression assays purchased from Applied Biosystems include Hs9999903\_m1 for beta-actin, Hs01110250\_m1 for HMOX1, Hs00359163\_s1 for HSPA1A, Hs00831826\_s1 for MT1A, and Hs00975960\_m1 for Nrf2, Hs00606316\_m1 for ACTC1, and Hs99999140\_m1 for FOS.

### Cytoprotection and cell proliferation assays

In order to assess relative cell proliferation and resistance to oxidative stress, HMEC-1 cells were passed at a 1:5 dilution and allowed to reattach to the plate overnight. Cells were then treated with HBOT or 100% O<sub>2</sub> at 1 atm, incubated for indicated times, and exposed to *t*-butyl hydroperoxide for 4 h. Cell proliferation was determined using the CellTiter96 Aqueous One Solution (Promega). This assay measures the conversion of MTS by metabolically active cells to a soluble formazan product, which is measured at 490 nm. Results are displayed with background subtracted and normalized to control, untreated samples.

### Vascular endothelial tube formation assay

Confluent HMEC-1 cells were treated with the HBOT protocol described above and then immediately plated on Matrigel-coated cell culture dishes (BD Biosciences, San Jose, CA) at a 1:1 passage in normal cell culture medium. Cells were incubated under normal conditions for 24 h and images were taken using 10 $\times$  objective on a Zeiss Axiovert 200 M microscope (Zeiss; Göttingen, Germany) using a Hamamatsu ORCA-ER camera (Hamamatsu; Bridgewater, NJ). For cultures that received two HBOT treatments, a 16-h recovery period at 37°C and normobaric conditions was allowed prior to the second treatment.

## Results

### HBOT and gene expression changes

To determine the impact of HBOT on gene regulation in human endothelial cells, Illumina bead arrays were performed on RNA extracted from HMEC-1 cells treated with HBO under conditions that approximate clinical settings (2.4 atm, 100% O<sub>2</sub>, 1 h). RNA expression was assessed in cells immediately following and 24 h after HBO exposure. To ensure that the microarray data were consis-

tent among biological replicates, scatterplots were constructed. Figure 1 illustrates that replicates in each of the groups have a very high correlation as indicated by the regression line and  $r^2$  values (0.99–1). In contrast, when expression values for CNTL0 were compared to HBOT0 or HBOT24, a broad scatter was observed, indicating numerous gene expression changes. Statistical analysis revealed

a total of 8,101 genes that were significantly regulated in at least one treatment level over control. Both increases and decreases in gene expression were observed compared to controls at each time point, with the majority of the changes taking place following the 24-h recovery (Fig. 2a). From these data, we selected genes that were increased or decreased by fivefold or more to be included as “top-

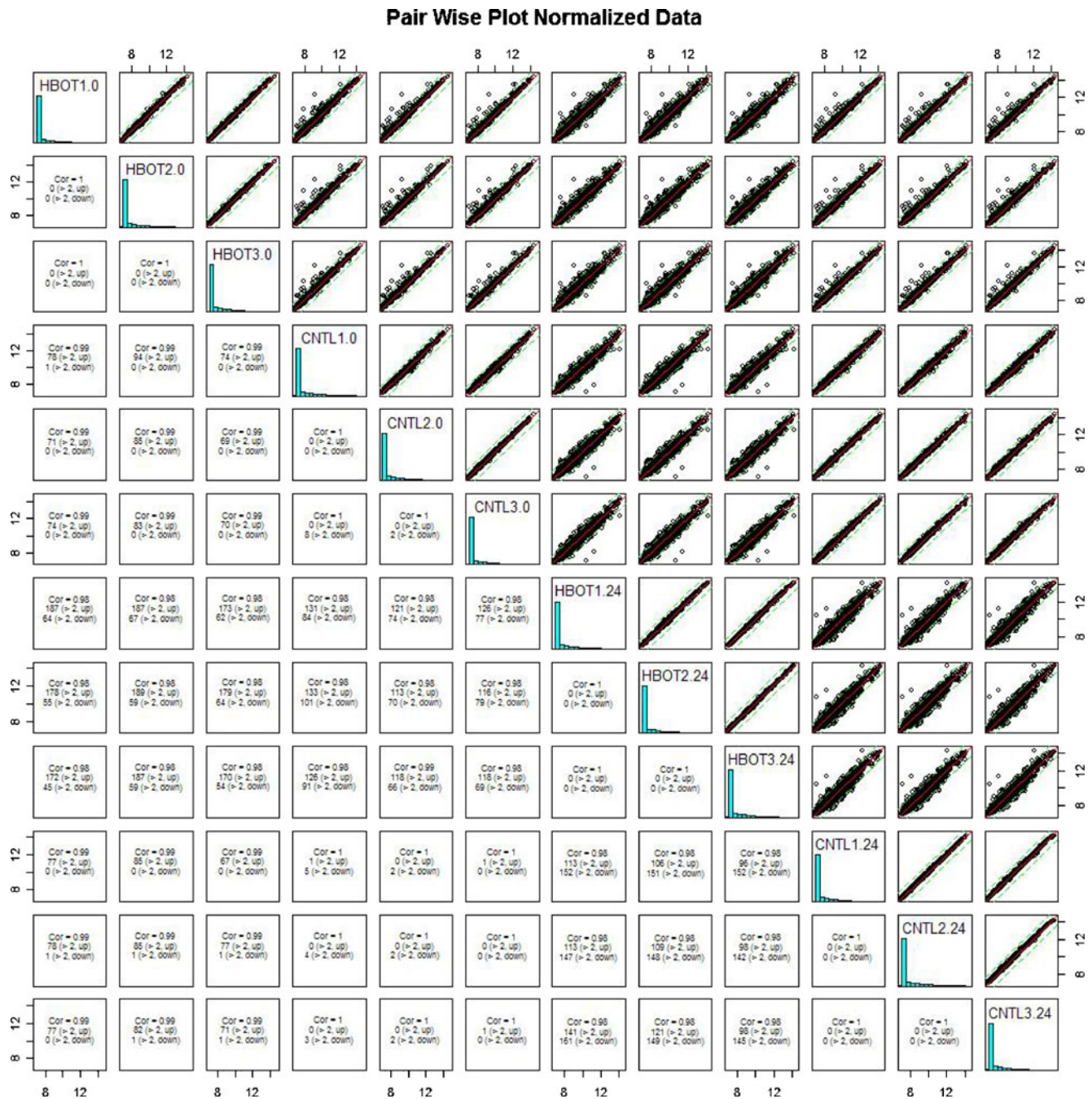


**Fig. 1** Scatterplots of normalized microarray data. These plots show the pairwise comparison of all 12 samples. *Graphs* represent the comparison of the normalized intensity data for every probe represented on the array between any two samples. The biological

triplicates exhibit very tight correlations serving as a quality control mechanism. Comparisons between HBOT-treated and HBOT-untreated samples show increased and decreased gene expression

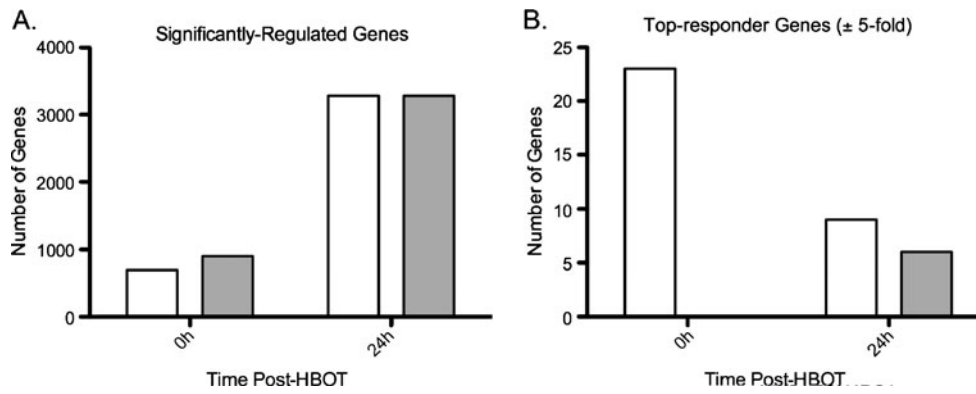


**Fig. 2** Microarray data analysis. **a** Differentially regulated genes were selected based on a significant difference in at least one treatment level compared to control. Following statistical analysis, a total of 8,101 (21%) significantly regulated genes were identified. Of that list, about 695 increased and 901 decreased immediately following HBOT,

whereas 3,280 increased and 3,968 decreased following the 24-h recovery. **b** Genes regulated  $\pm 5$ -fold were selected as top-responding genes. *White bars* indicate up-regulated genes; *gray bars* indicate down-regulation

responders.” Figure 2b depicts the results of this selection. Although more overall gene expression changes occurred at the 24-h time point, most of the top-responder gene expression changes were observed immediately following HBOT. Gene details of this list are shown in Tables 1 and 2.

One of our interests is the potential usefulness of HBOT as a preconditioning stress to induce cytoprotective gene

expression. We therefore examined the effects of HBOT on several molecular chaperone genes present on the array, as shown in Table 3. Chaperone genes [heat shock protein (HSP) and DNAJ related] shown in the table were selected from the list of significantly regulated genes having a fold change above or below 1.25. These data indicate that a number of molecular chaperones were up-regulated imme-

**Table 1** Top-responding genes immediately after HBOT

Official symbol	Official gene name	GeneID	HBOT-0h/CNTL-0h
FOSB	FBJ murine osteosarcoma viral oncogene homolog B	2354	38.7
MT1X	Metallothionein 1X	4501	34.69
MT1G	Metallothionein 1G	4495	29.5
FOS	BJ murine osteosarcoma viral oncogene homolog	2353	24.57
NR4A2	Nuclear receptor subfamily 4, group A, member 2	4929	22.72
RASD1	RAS, dexamethasoneinduced 1	51655	16.72
EGR1	Early growth response 1	1958	11.74
EGR2	Early growth response 2	1959	11.25
SERTAD1	SERTA domain containing 1	29950	10.6
SNF1LK	SNF1-like kinase	54018	10.23
MT1H	Metallothionein 1H	4496	10.2
MT1M	Metallothionein 1 M	4499	9.25
JUNB	jun B proto-oncogene	3726	8.92
MT1F	Metallothionein 1F	4494	8.63
AXUD1	Cysteine-serine-rich nuclear protein 1	64651	8.5
HES1	Hairy and enhancer of split 1, (Drosophila)	3280	7.81
SLC30A1	Solute carrier family 30 (zinc transporter), member 1	7779	7.43
BHLHB2	Basic helix-loop-helix family, member e40	8553	7.42
MT1E	Metallothionein 1E	4493	6.42
KLF10	Kruppel-like factor 10	7071	6.34
MT1P3	Metallothionein 1 pseudogene 3	140851	6.28
IL11	Interleukin 11	3589	5.69
ACTC1	Actin, alpha, cardiac muscle 1	70	5.17

**Table 2** Top-responding genes 24-h post-HBOT

Official symbol	Official gene name	GeneID	HBOT24/CNTL24
MT1H	Metallothionein 1h	4496	50.00
MT1X	Metallothionein 1x	4501	16.67
MT1F	Metallothionein 1f	4494	12.50
LIPG	Lipase, endothelial	9388	12.50
MT1P3	Metallothionein 1 pseudogene 3	140851	8.33
MT1E	Metallothionein 1e	4493	7.14
ENDOGL1	Endo/exonuclease (5'-3'), endonuclease g-like	9941	5.88
SLCO2A1	Solute carrier organic anion transporter family, member 2A1	6578	5.26
GAL	Galanin prepropeptide	51083	5.00
GDF15	Growth differentiation factor 15	9518	-8.87
KLHL24	Kelch-like 24 ( <i>Drosophila</i> )	54800	-6.7
C5orf26	Chromosome 5 open reading frame 26	114915	-5.76
ABCA1	ATP-binding cassette, subfamily A (ABC1), member 1	19	-5.43
PSG4	Pregnancy specific beta-1-glycoprotein 4	5672	-5.36
HSPA5	Heat shock 70 kDa protein 5 (glucose-regulated protein, 78 kDa)	3309	-5.07

diately following HBOT, with a number of changes persisting through 24 h. A small subset of chaperone genes were down-regulated at 24-h post-HBOT, which may result from a feedback inhibition from the early HSP activation (Yura et al. 2007; Zhang and Andersen 2007).

#### Biological function analysis

In order to obtain insight into which biological processes are most relevant to the gene list, genes that were significantly up-regulated by 1.25-fold or more or down-regulated by 0.75-fold or more were uploaded into the Ingenuity Pathway Analysis software. For functional analysis, the software selects genes that are enriched within a particular biological category and assigns a *p* value based on the enrichment number in comparison to the entire Ingenuity knowledge base. For our analysis, we selected results with highly significant *p* values ( $\leq 0.001$ ) as described in the “Materials and Methods.” Table 4 displays the results of this analysis showing the top 5 regulated functions (full lists are available in Supplementary Tables 1 and 2). In general, the same categories are represented at both the 0- and 24-h time points. This analysis predicts that HBOT impacts the cell cycle, cell movement, and morphology as well as gene expression/regulation and cell growth, proliferation, and death.

#### Pathway analysis

In order to gain insight into which specific cellular pathways might be affected by HBOT, we examined the pathway results generated from the Ingenuity software. One

pathway of particular interest to us that was found to be significantly affected was the Nrf-2 oxidative stress response pathway. Figure 3 illustrates the gene expression changes detected in this pathway. Nrf-2 is a transcription factor that binds the antioxidant response elements of gene promoters in a complex with macrophage activating factor (MAF). The expression both Nrf-2 and MAF mRNAs were increased following HBO exposure, as were a number of Nrf-2 target genes (including metallothionein, heme oxygenase, and thioredoxin). Although the changes associated with this pathway were complex with both positive and negative acting changes ensuing, the increased expression of target genes is consistent with an overall stimulation of this pathway. As described below, HBOT also protected cells from oxidant stress, which is likewise consistent with an activation of this pathway.

#### Validation and expansion of microarray data

In order to validate some of the changes described by the microarray, we chose to use quantitative PCR (qPCR) and Taqman reagents. To date, most hyperbaric studies do not compare HBOT results to the effects of high oxygen treatment alone, so we addressed this issue by treating the HMEC-1 cells with 100% O<sub>2</sub> at 1 atm for 1 h within the same chamber used for the hyperbaric studies. Furthermore, we wished to expand our time course studies in order to clarify the kinetics of gene activation following HBOT or 100% O<sub>2</sub>. Figure 4 shows the results of these studies. For all of the genes tested, HBOT was required to elicit the highest degree of activation and changes were found to be minimal following 100% O<sub>2</sub> treatment at 1 atm. For some

**Table 3** Chaperone genes affected by HBOT

Official symbol	Official gene name	GeneID	HBOT-0h/ CNTL-0h	HBOT-24h/ CNTL-24h
DNAJB1	DnaJ (Hsp40) homolog, subfamily B, member 1	3337	1.83	
HSPA1B	Heat shock 70 kDa protein 1B	3304	1.81	
HSPA1A	Heat shock 70 kDa protein 1A	3303	1.73	
HSPH1	Heat shock 105 kDa/110 kDa protein 1	10808	1.49	
SERPINH1	Serpin peptidase inhibitor, clade H (heat shock protein 47), member 1, (collagen binding protein 1)	871	1.4	
HSPA2	Heat shock 70 kDa protein 2	3306	1.34	
DNAJ4	DnaJ (Hsp40) homolog, subfamily A, member 4	55466	1.32	
DNAJC11	DnaJ (Hsp40) homolog, subfamily C, member 11	55735		2.04
HSPA14	Heat shock 70 kDa protein 14	51182		1.96
HSPE1	Heat shock 10 kDa protein 1 (chaperonin 10)	3336		1.96
HSPH2	Heat shock 70 kDa protein 4	3308		1.92
HSPH1	Heat shock 105 kDa/110 kDa protein 1	10808		1.82
HSPC3	Heat shock protein 90 kDa alpha (cytosolic), class B member 1	3326		1.72
TCP1	t-complex 1	6950		1.72
DNAJC7	DnaJ (Hsp40) homolog, subfamily C, member 7	7266		1.59
DNAJC17	DnaJ (Hsp40) homolog, subfamily C, member 17	55192		1.54
DNAJC3	DnaJ (Hsp40) homolog, subfamily C, member 3	5611		1.54
DNAJC5	DnaJ (Hsp40) homolog, subfamily C, member 5	80331		1.47
DNAJC19	DnaJ (Hsp40) homolog, subfamily C, member 19	131118		1.45
HSPD1	Heat shock 60 kDa protein (chaperonin)	3329		1.45
SERPINH1	Serpin peptidase inhibitor, clade H (heat shock protein 47), member 1, (collagen binding protein 1)	871		1.44
DNAJA1	DnaJ (Hsp40) homolog, subfamily A, member 1	3301		1.39
HSPA8	Heat shock 70 kDa protein 8	3312		1.27
HSPA1A	Heat shock 70 kDa protein 1A	3303		-1.39
DNAJB11	DnaJ (Hsp40) homolog, subfamily B, member 11	51726		-1.4
HSPA2	Heat shock 70 kDa protein 2	3306		-1.4
HSPBAP1	HSPB (heat shock 27 kDa) associated protein 1	79663		-1.58
DNAJC18	DnaJ (Hsp40) homolog, subfamily C, member 18	202052		-1.61
HSP90B1	Heat shock protein 90 kDa beta (Grp94), member 1	7184		-1.69
DNAJB9	DnaJ (Hsp40) homolog, subfamily B, member 9	4189		-3.4
HSPA5	Heat shock 70 kDa protein 5 (glucose-regulated protein, 78 kDa)	3309		-5.07

of the genes examined (Nrf2, HSPA1A, MT1A, and FOS), 100% O<sub>2</sub> treatment was not sufficient to activate gene expression above control levels. Maximal activation for HMOX1, Nrf2, HSPA1A, and ACTC1 occurred at 4 h post-treatment, while two of the genes FOS and MT1A were maximally activated immediately following HBOT.

#### Functional relevance of gene expression changes

The gene expression analysis indicated potential changes in cell proliferation (Table 3), cell survival (Table 3), and oxidant protection through the Nrf-2 antioxidant pathway (Fig. 3). We therefore performed experiments to determine the functional relevance of these gene expression changes.

We first tested the ability of HBO to protect cells from oxidative stress. In this experiment, HMEC-1 cells were preconditioned with HBO and then treated with *t*-butyl hydroperoxide to induce oxidative stress. As shown in Fig. 5a, cells exposed to HBOT showed a greater resistance to oxidative stress than control cells. HBOT was also more effective at preconditioning cells than 100% O<sub>2</sub> at 1 atm, supporting an important role of increased pressure in achieving this protection. Since the gene array data suggested potential changes in cell proliferation, we also determined the effect of HBOT on cell number 24 h after HBO exposure. As shown in Fig. 5b, HBOT increased the number of viable cells in the culture at the 24-h time point. This enhanced proliferation also required elevated pressure

**Table 4** Top 5 biological functions affected by HBOT

Function	Percentage <sup>a</sup>
HBOT-0 h	
Cellular growth and proliferation	40.9
Cell death	39.1
Gene expression	33.8
Cellular development	18.1
Cell morphology	16.0
HBOT-24 h	
Cell growth and proliferation	31.7
Cell death	26.6
Gene expression	18.1
Cell cycle	13.2
Cellular compromise	13.0

<sup>a</sup> Percentage of genes identified within a specific category out of the total number of genes determined to be present as a significantly affected biological function in all categories

and was not observed following treatment with 100% O<sub>2</sub> at 1 atm alone.

Finally, because some of the HBOT-induced changes occurred in genes regulating cell migration, cell morphology, and proliferation, we also assessed the impact of HBOT on the ability of HMEC-1 cells to form microvascular tube structures. For these studies, we took advantage of the propensity of HMEC-1 cells to spontaneously form tubes that resemble primary vasculature when plated on Matrigel (Ades et al. 1992). Cells were treated with or without HBOT and then plated on Matrigel. Cells received either one or two HBO treatments. The results are displayed in Fig. 5c. It is apparent that, after a single HBO treatment, tube formation occurred more readily than in control. Tube formation was further enhanced with an additional HBOT applied 16 h after the first. In contrast, cells treated with 100% O<sub>2</sub> at 1 atm showed no improvement in vascular network formation compared to controls with one or two treatments (data not shown). Although the mechanism underlying the enhanced response to the second HBO treatment is still unclear, this finding supports the possibility that the cellular changes induced by an initial HBOT may prime cells for the second exposure. Furthermore, repeated treatments are commonly used clinically, and we are interested in exploring the cellular response to multiple treatments.

## Discussion

To understand the molecular changes that occur in endothelial cells following HBOT, we explored global gene

**Fig. 3** HBOT affects gene expression in the Nrf2 Pathway. Ingenuity Pathway Analysis predicted the Nrf2-mediated oxidative stress response pathway as having significantly changed gene expression for both time points. Molecules are divided into right (HBOT-0 h) and left (HBOT-24 h) halves. *Red color* indicates up-regulation, *green* indicates down-regulation, and *white* indicates no change in comparison to control

expression changes using a microarray approach. We found 8,101 genes to be significantly regulated either immediately following HBOT or after a 24-h recovery period. Of these statistically significant genes, we examined which genes were changing to the highest degree. Some important top responders that are up-regulated immediately by HBOT include the immediate early transcription factors, FOS, FOSB, and JUNB, which may be indicative of enhanced proliferation potential (Pahl and Baeuerle 1994; Asakuno et al. 1995; Shono et al. 1996). Other top-responding genes that are up-regulated at both time points include the metallothionein family of proteins, which are known to protect against oxidative stress (Bell and Vallee 2009). Although the array analysis suggests that a number of endothelial cell signaling pathways may be altered by HBOT, we focused much of our analysis on proliferation and protective responses.

HBOT can protect cells against lethal heat stress and has been reported to extend the lifespan of some model organisms (Cypser and Johnson 2002). Furthermore, it has been shown that pretreatment with HBO can reduce cognitive decline following coronary artery bypass graft surgery in humans (Cypser and Johnson 2002; Alex et al. 2005). Consistent with these observed physiological effects, we found that HBOT does increase the expression of molecular chaperones in microvascular endothelial cells at both time points examined. Although these were not among the top-responding genes, ranging from the lowest stimulation at 1.27-fold to a high of 2.04-fold, up to 20 genes in this category were activated. Interestingly, abundant cellular proteins like molecular chaperones are typically not induced to very high fold-increases but are still capable of eliciting a response within the cell (Hageman 2008). While it is not yet clear what specific function these chaperones have in endothelial cells, our functional data would suggest that they might play a role in protecting cells from lethal oxidative stress (Fig. 5). In addition, we see down-regulation of some molecular chaperones at the 24-h time point including HSPA1A and HSPA2. The mRNA encoding HSPA1A is known to be transiently elevated in stressed cells due to the activation of a negative feedback loop (Theodorakis et al. 1999), and this feedback control may be in operation 24 h post-HBOT. Four of the down-regulated genes encode endoplasmic reticulum (ER) luminal proteins that are involved with protein folding, DNAJB11, HSP90B1,

NRF2-mediated Oxidative Stress Response

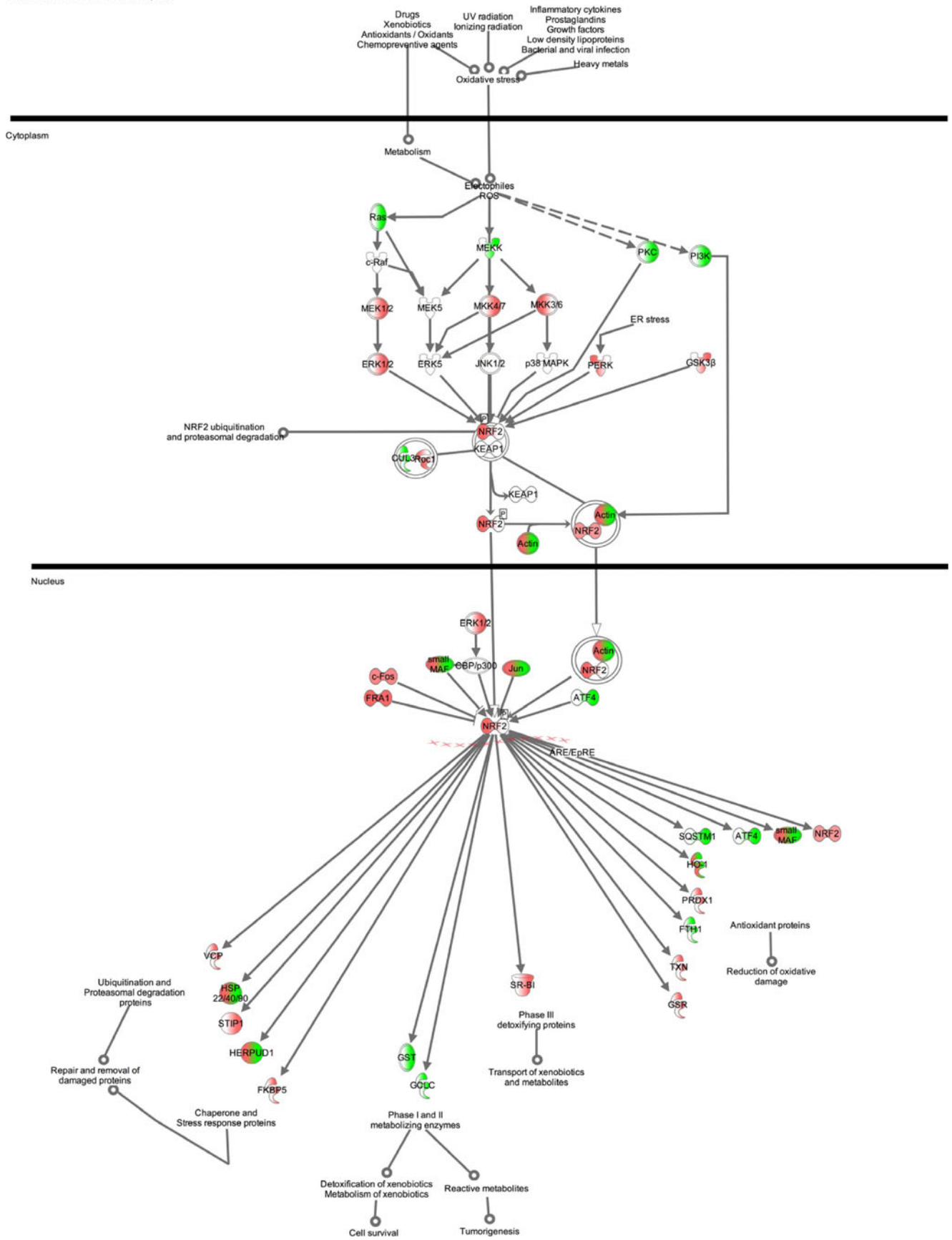
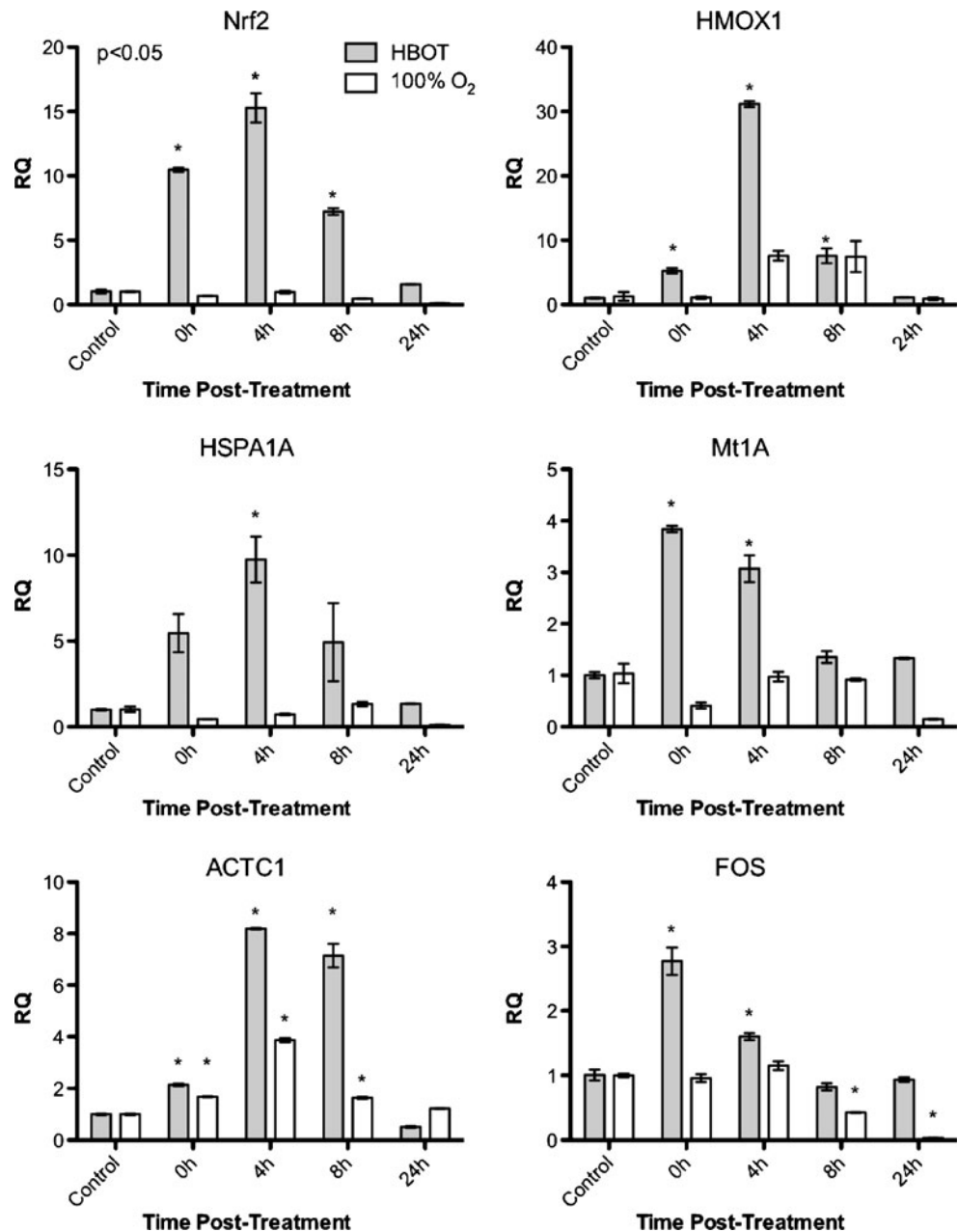


**Fig. 4** Validation of microarray data. HMEC-1 cells were treated with either HBOT or 100% O<sub>2</sub> and RNA extracted at indicated times following treatment. RNA was converted to cDNA and subjected to qPCR for the indicated genes. Genes were selected from pathways of interest including the Nrf2 signaling pathway, cytoprotective genes, and the top-responding genes. *HMOX1* heme-oxygenase 1, *HSPA1A* human heat shock protein 70, *Mt1A* metallothionein 1 A, *ACTC1* actin, alpha cardiac muscle 1, *FOS* FBJ murine osteosarcoma viral oncogene homolog



DNAJB9, and HSPA5. This might indicate a decrease in the activity of the ER/Golgi pathway (Schroder and Kaufman 2005). While further investigation is needed into which specific molecular chaperones may be acting in these cells under our HBOT conditions, it is apparent that HBOT can induce the expression of key protective genes, providing evidence for the use of HBOT as such a preconditioning stress.

Ingenuity Pathway Analysis predicted some interesting cellular changes following HBOT. In general, genes categorized in cell growth and proliferation, cell death, and gene expression were among the top affected functional categories. Giving a general sense of affected functions, these data can help to predict mechanisms that are involved

in HBOT-induced processes, specifically wound healing, as well as suggest some potential new applications of the treatment. While it is known that HBOT can stimulate growth of several cell types, the specific underlying genes have not been studied. Our data confirm that HBOT can induce cell growth in microvascular endothelial cells and point to the subunits of the AP-1 transcription factor as playing a role. While further studies need to be completed to verify the role of these genes, this dataset has revealed potential candidate mechanisms.

With regard to endothelial cell protection, pathway analysis pointed to the Nrf-2 oxidative stress response pathway as being an important pathway regulated by HBOT. This pathway controls the expression of over 200 protective and

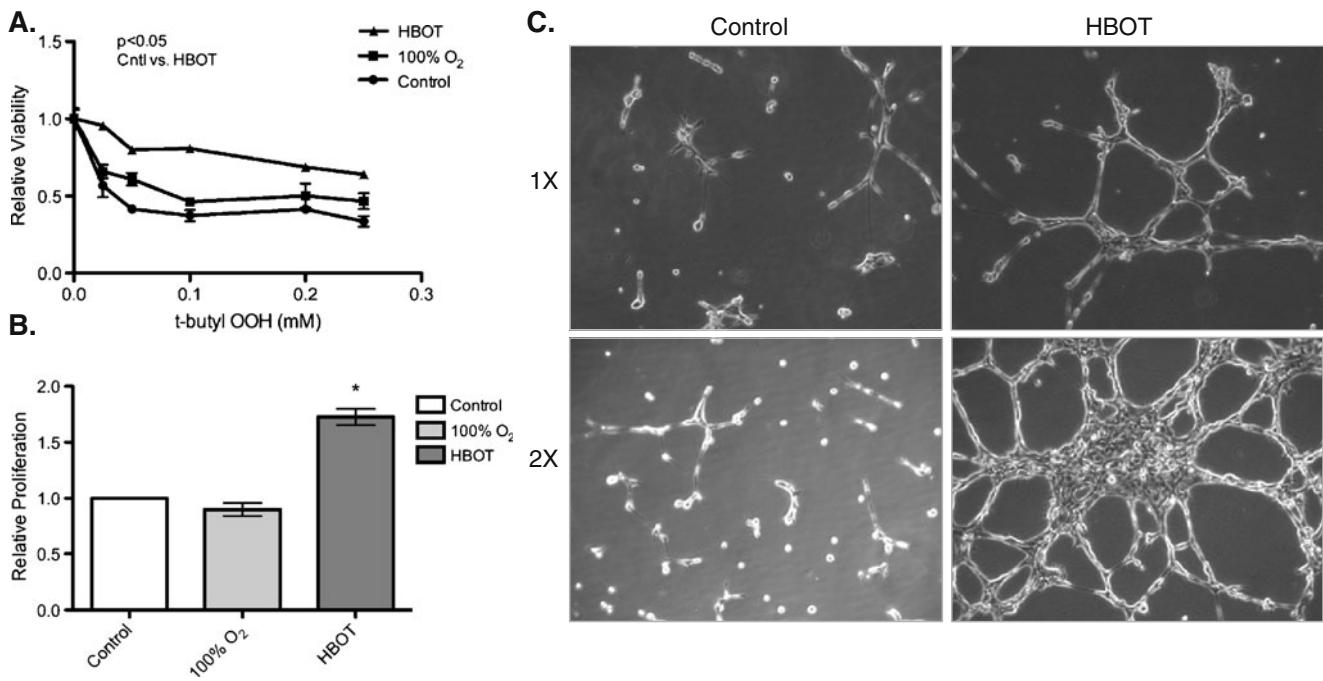


**Fig. 5** Functional effects of HBOT and 100% O<sub>2</sub> on HMEC-1 cells. Cells were plated and incubated for 48 h before being subjected to one round of HBOT or 100% O<sub>2</sub>. Following recovery for 16 h, cell proliferation was assessed with the MTT assay. **a** HBOT protected against oxidative stress. Following recovery from HBOT or 100% O<sub>2</sub>, cells were treated with *t*-butylhydroperoxide (*t*-butyl OOH) for 4 h and then analyzed for cell viability using the MTT assay. **b** HBOT

increased cell viability. **c** HBOT increased vascular tube formation. HMEC-1 cells received either one (1X) or two (2X) treatments separated by a 24-h recovery period of HBOT and were immediately plated on Matrigel coated plates. Representative images are shown for control samples (**c** 1X and C 2X) as well as HBOT cells treated once or twice (HBOT 1X and HBOT 2X)

antioxidant genes (Suh et al. 2004; Nguyen et al. 2009; Zakkar et al. 2009). Our data indicate that HBOT can induce the expression of a number of Nrf-2 target genes, and it is likely that these genes are contributing to the protection of the endothelial cells to oxidative stress (Fig. 5). Metallothioneins, which are among the top-responders to HBOT, can be regulated by Nrf-2 (Ohtsuji et al. 2008). One particularly interesting Nrf-2-regulated gene activated by HBOT is the heme oxygenase gene, HMOX1. HMOX1 is up-regulated by 3.72-fold immediately following HBOT and remains elevated by 1.44-fold after 24 h recovery. Since HMOX1 reaction products are known to provide cytoprotection from inflammatory diseases, including atherosclerosis, HMOX1 induction may play an important role in providing some of the clinically beneficial effects of HBOT (Ryter et al. 2006). In general, induction of the Nrf-2 pathway is likely to provide a range of anti-inflammatory and other health benefits (Al-Waili and Butler 2006; Osburn and Kensler 2008).

Given the general pro-growth and pro-survival actions of HBOT on the endothelial cells and the fact that genes involved in cell mobility were affected by HBOT, we assessed the impact of HBOT on the ability of cells to form a vascular network. We found that a single HBOT enhanced network formation of these cells and that two daily

treatments performed even better. Although the mechanism underlying the enhanced response to the second HBO treatment is still unclear, this finding supports the possibility that the cellular changes induced by an initial HBOT may further predispose endothelial cells to the pro-growth and maturation effects of a second treatment.

In summary, we find that HBOT activated the expression of cytoprotective and growth-promoting genes in endothelial cells. This response was dependent on elevated pressure, indicating that high concentrations of dissolved oxygen were required to induce these responses. In addition, HBOT was found to enhance endothelial cell vascular network formation, particularly after two successive treatments. The molecular effects we report here provide mechanistic insight into the cellular changes induced by HBOT and offer an opportunity to generate more hypotheses. These molecular responses may be useful in understand and improving clinical applications of HBOT.

**Acknowledgements** We would like to thank OxyHeal Health Group for providing the funding and hyperbaric chamber for these studies. We would also like to extend our gratitude to Alexandria Thornton and Bryan Lawlor for their work during the early stages of the project. We would like to thank Advanced Turbine Services, LLC for donating some of the equipment used in this work. For technical support, we thank Dr. Carol Norris, Facility Scientist at the University of Connecticut FCCM Facility.

## References

- Ades EW, Candal FJ, Swerlick RA, George VG, Summers S, Bosse DC, Lawley TJ (1992) HMEC-1: establishment of an immortalized human microvascular endothelial cell line. *J Invest Dermatol* 99:683–690
- Alex J, Laden G, Cale AR et al (2005) Pretreatment with hyperbaric oxygen and its effect on neuropsychometric dysfunction and systemic inflammatory response after cardiopulmonary bypass: a prospective randomized double-blind trial. *J Thorac Cardiovasc Surg* 130:1623–1630
- Al-Waili NS, Butler GJ (2006) Effects of hyperbaric oxygen on inflammatory response to wound and trauma: possible mechanism of action. *ScientificWorldJournal* 6:425–441
- Asakuno K, Isono M, Wakabayashi Y, Mori T, Hori S, Kohno K, Kuwano M (1995) The exogenous control of transfected c-fos gene expression and angiogenesis in cells implanted into the rat brain. *Brain Res* 702:23–31
- Bell SG, Vallee BL (2009) The metallothionein/thionein system: an oxidoreductive metabolic zinc link. *ChemBioChem* 10:55–62
- Cypser JR, Johnson TE (2002) Multiple stressors in *Caenorhabditis elegans* induce stress hormesis and extended longevity. *J Gerontol A Biol Sci Med Sci* 57:B109–B114
- Du P, Kibbe WA, Lin SM (2008) lumi: a pipeline for processing Illumina microarray. *Bioinformatics* 24:1547–1548
- Duzgun AP, Satir HZ, Ozozan O, Saylam B, Kulah B, Coskun F (2008) Effect of hyperbaric oxygen therapy on healing of diabetic foot ulcers. *J Foot Ankle Surg* 47:515–519
- Efrati S, Gall N, Bergan J et al (2009) Hyperbaric oxygen, oxidative stress, NO bioavailability and ulcer oxygenation in diabetic patients. *Undersea Hyperb Med* 36:1–12
- Gesell LB (2008) Hyperbaric oxygen therapy indications, 12th edn. Undersea and Hyperbaric Medical Society, Durham
- Godman CA, Joshi R, Tierney BR et al (2008) HDAC3 impacts multiple oncogenic pathways in colon cancer cells with effects on Wnt and vitamin D signaling. *Cancer Biol Ther* 7:1570–1580
- Gurdol F, Cimsit M, Oner-Iyidogan Y, Kocak H, Sengun S, Yalcinkaya-Demirsoz S (2009) Collagen synthesis, nitric oxide and asymmetric dimethylarginine in diabetic subjects undergoing hyperbaric oxygen therapy. *Physiol Res* 2009 Aug 12 (Epub ahead of print)
- Hageman J (2008) The human HSP70/HSP40 chaperone family: a study on its capacity to combat proteotoxic stress. PhD thesis, Department of Cell Biology, University Medical Center Groningen, Groningen, p. 188
- Ihaka R, Gentleman R (1996) R: a language for data analysis and graphics. *J Comput Graph Stat* 5:16
- Li Q, Li J, Zhang L, Wang B, Xiong L (2007) Preconditioning with hyperbaric oxygen induces tolerance against oxidative injury via increased expression of heme oxygenase-1 in primary cultured spinal cord neurons. *Life Sci* 80:1087–1093
- Liu ZJ, Velazquez OC (2008) Hyperoxia, endothelial progenitor cell mobilization, and diabetic wound healing. *Antioxid Redox Signal* 10:1869–1882
- Milovanova TN, Bhopale VM, Sorokina EM, Moore JS, Hunt TK, Hauer-Jensen M, Velazquez OC, Thom SR (2009) Hyperbaric oxygen stimulates vasculogenic stem cell growth and differentiation in vivo. *J Appl Physiol* 106:711–728
- Nguyen T, Nioi P, Pickett CB (2009) The Nrf2-antioxidant response element signaling pathway and its activation by oxidative stress. *J Biol Chem* 284:13291–13295
- Ohtsuji M, Katsuoaka F, Kobayashi A, Aburatani H, Hayes JD, Yamamoto M (2008) Nrf1 and Nrf2 play distinct roles in activation of antioxidant response element-dependent genes. *J Biol Chem* 283:33554–33562
- Ong M (2008) Hyperbaric oxygen therapy in the management of diabetic lower limb wounds. *Singapore Med J* 49:105–109
- Osburn WO, Kensler TW (2008) Nrf2 signaling: an adaptive response pathway for protection against environmental toxic insults. *Mutat Res* 659:31–39
- Pahl HL, Baeuerle PA (1994) Oxygen and the control of gene expression. *Bioessays* 16:497–502
- Ren P, Kang Z, Gu G et al (2008) Hyperbaric oxygen preconditioning promotes angiogenesis in rat liver after partial hepatectomy. *Life Sci* 83:236–241
- Rothfuss A, Speit G (2002) Investigations on the mechanism of hyperbaric oxygen (HBO)-induced adaptive protection against oxidative stress. *Mutat Res* 508:157–165
- Ryter SW, Alam J, Choi AM (2006) Heme oxygenase-1/carbon monoxide: from basic science to therapeutic applications. *Physiol Rev* 86:583–650
- Sander AL, Henrich D, Muth CM, Marzi I, Barker JH, Frank JM (2009) In vivo effect of hyperbaric oxygen on wound angiogenesis and epithelialization. *Wound Repair Regen* 17:179–184
- Schroder M, Kaufman RJ (2005) The mammalian unfolded protein response. *Annu Rev Biochem* 74:739–789
- Shono T, Ono M, Izumi H, Jimi SI, Matsushima K, Okamoto T, Kohno K, Kuwano M (1996) Involvement of the transcription factor NF-kappaB in tubular morphogenesis of human microvascular endothelial cells by oxidative stress. *Mol Cell Biol* 16:4231–4239
- Speit G, Denog C, Eichhorn U, Rothfuss A, Kaina B (2000) Induction of heme oxygenase-1 and adaptive protection against the induction of DNA damage after hyperbaric oxygen treatment. *Carcinogenesis* 21:1795–1799
- Suh JH, Shenvi SV, Dixon BM, Liu H, Jaiswal AK, Liu RM, Hagen TM (2004) Decline in transcriptional activity of Nrf2 causes age-related loss of glutathione synthesis, which is reversible with lipoic acid. *Proc Natl Acad Sci U S A* 101:3381–3386
- Thackham JA, McElwain DL, Long RJ (2008) The use of hyperbaric oxygen therapy to treat chronic wounds: A review. *Wound Repair Regen* 16:321–330
- Theodorakis NG, Drujan D, De Maio A (1999) Thermotolerant cells show an attenuated expression of Hsp70 after heat shock. *J Biol Chem* 274:12081–12086
- Thom SR (2009) Oxidative stress is fundamental to hyperbaric oxygen therapy. *J Appl Physiol* 106:988–995
- Yuan J, Handy RD, Moody AJ, Bryson P (2009) Response of blood vessels in vitro to hyperbaric oxygen (HBO): modulation of VEGF and NO(x) release by external lactate or arginine. *Biochim Biophys Acta* 1787:828–834
- Yura T, Guisbert E, Poritz M, Lu CZ, Campbell E, Gross CA (2007) Analysis of sigma32 mutants defective in chaperone-mediated feedback control reveals unexpected complexity of the heat shock response. *Proc Natl Acad Sci U S A* 104:17638–17643
- Zakkar M, Van der Heiden K, Luong LA et al (2009) Activation of Nrf2 in endothelial cells protects arteries from exhibiting a proinflammatory state. *Arterioscler Thromb Vasc Biol* 29:1851–1857
- Zhang Q, Andersen ME (2007) Dose response relationship in anti-stress gene regulatory networks. *PLoS Comput Biol* 3:e24
- Zhang Q, Chang Q, Cox RA, Gong X, Gould LJ (2008) Hyperbaric oxygen attenuates apoptosis and decreases inflammation in an ischemic wound model. *J Invest Dermatol* 128:2102–2112